

Received October 19, 2019, accepted November 3, 2019, date of publication December 12, 2019, date of current version January 8, 2020.

Digital Object Identifier 10.1109/ACCESS.2019.2959082

Optimal Trajectory Planning of Electromagnetic Valve-Train Based on Multiple Algorithms for Improving Engine Performance

TONGJUN GUO¹, SIQIN CHANG¹, AND JIANGTAO XU²

¹School of Mechanical Engineering, Nanjing University of Science and Technology, Nanjing 210094, China

²School of Mechanical Engineering, Nanjing Institute of Technology, Nanjing 211167, China

Corresponding author: Tongjun Guo (gtj0731@163.com)

This work was supported by the National Natural Science Foundation of China under Grant 51306090.

ABSTRACT Electromagnetic valve-train (EMVT) is a camless variable valve technology that can adjust the valve movement state independently, continuously and in real time. It can adjust the engine charge efficiency according to engine working conditions. In this paper, in order to achieve the optimal inflation efficiency, a new-style moving-coil electromagnetic linear actuator (ELA) was designed and genetic algorithm (GA) was used to plan the valve motion trajectory in common working conditions. Furthermore, an improved BP neural network algorithm was used to optimize the valve operation mode in all working conditions. The new valve operation scheme was applied to the modified intake system of engine, and its simulation and test analysis were carried out. Compared with the prototype, the results showed that the charging efficiency was greatly improved in the range of full rotating speed, especially in the range of middle and low rotating speed up to 95.6%.

INDEX TERMS Electromagnetic valve-train, genetic algorithm, neural network, grey relational analysis, optimal trajectory planning.

I. INTRODUCTION

With the continued growth of the economy, the demand for automobiles has further increased, and the huge car ownership has brought severe energy and environmental problems. Carbon, NO_x and other substances in automobile emissions seriously affect urban air quality and bring harm to people's health. Therefore, energy conservation and environmental protection are urgent issues in the automotive industry.

New energy vehicles are an important goal of the current automobile industry. However, in the transition period, traditional internal combustion engine vehicles still occupy the majority of the market share [1], so it has more practical significance for traditional automobile to save energy and reduce emission. Now, many automobile manufacturers and research institutes have been optimizing and improving the technology of internal combustion engines to further reduce vehicle fuel consumption and emissions technologies [2]–[8], mainly in the following aspects:

The associate editor coordinating the review of this manuscript and approving it for publication was Xiaosong Hu¹.

a. engine management system(EMS). It usually consists of various sensors to monitor the real-time operating conditions of the engine and control the operations such as ignition, air-fuel ratio, idle speed and complex variable valve timing, etc. In EMS, advanced control strategies can be adopted to reduce emissions, improve fuel economy and engine performance. Ashok *et al.* [2] introduce the commonly control modules in the EMS: torque control module, air-fuel ratio control module, electronic throttle control module, idle control module, ignition control module, knock detection and control module and diagnostic system module. At the same time, the development prospect of engine control system is presented. For example, an “open architecture” based EMS was developed in which control algorithm can be added, replaced or modified with plug and play features. The sensor fusion techniques is adopted to obtain lower detection error probability and higher reliability. The intelligent control EMS system is developed to realize real-time monitoring, remote diagnosis, online analysis and prevention. Ashok *et al.* [3] introduce the model of electronic throttle control system of engine and its existing control methods in detail.

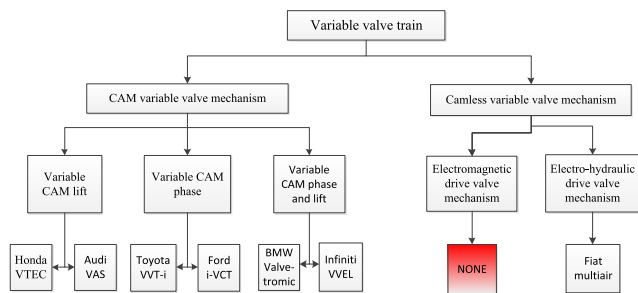


FIGURE 1. Types of variable valve-train.

The electronic throttle control system can accurately control the throttle angle according to the requirements of the driver and other systems with advanced control strategies, so as to change the air inlet velocity. Ashok [4] proposes an integrated electronic throttle control algorithm based on accurate estimation of throttle angle based on pedal follower and torque. The above methods can be adopted to improve the fuel economy and emission performance of the engine.

b. Turbocharging technology. It improves the power performance by increasing the intake density, and at the same time brings low-emission, reduces the pumping loss of the engine, and improves the fuel economy of the engine [5]–[8]. Petitjean *et al.* [5] analyze and compare turbocharged and non-turbocharged engines. The results show that for the same power turbocharging can reduce the volume of gasoline engine by about 30%, and improve fuel economy by 8-10% while improving torque and acceleration performance.

c. Variable valve-train technology. The cam-driven variable valve-train technology can adopt different valve opening periods and lifts under different working conditions, which is beneficial to improving the charging efficiency and combustion effect of the engine. As shown in Fig. 1, Variable Valve Timing (VVT) and Variable Valve Lift (VVL) [9]–[13]. These technologies have been widely used in automotive products, but the cam-driven variable valve-train technology still has a lot of room for improvement due to the limitation of the cam profile. Hong *et al.* [10] introduce the literature in the technology of intake and exhaust philosophies of VVT and analyzed the effects of different VVT methods on single-cylinder engine by the GT-Power software. Fujita *et al.* [13] introduce the variable valve actuation system (VVEL) developed by Nissan Motor Company and its application in detail. The results show that it had substantially enhanced engine performance attributes, namely, fuel economy, exhaust emissions, and engine output.

d. Start-Stop technology. It is also known as variable displacement technology. When the engine is running under partial load conditions, some cylinders will be stopped, and the load rate of the remaining cylinders will be added to maintain the power performance, so that the whole engine works in the high load areas which have higher efficiency. This technology can increase engine efficiency and reduce fuel consumption [17], [18]. Qiao *et al.* [17] introduce the structure, relation components, operational principle and application of

intelligent engine start-stop system. Through a large number of comparative tests, the intelligent engine start-stop system can improve fuel consumption and reduce part of emission.

e. Variable compression ratio technology. Generally, the compression ratio of the engine is fixed, and does not exceed 11:1. If the compression ratio exceeds the ultimate value, it is easy to cause knocking under heavy load conditions and sacrifice part of energy at low load conditions, so adjusting the compression ratio according to engine operating conditions can improve the fuel economy of the engine [19]–[21]. Shaik *et al.* [19] review the geometric approaches and solutions are used to achieve VCR, consider the results of prior research, and forecast the benefits of VCR for present engine design.

However, due to the complicated structure, the difficulty of processing, the wear and sealing of components, the precision of electronic control and other technical problems, the application of variable compression ratio technology in automobile engines is limited.

f. Lean burn technology. Through lean burn mixture (air-fuel ratio greater than 18), the key technology is to achieve stratified combustion to improve fuel economy [22], [23]. Horie *et al.* [23] describe the development of a four-valve lean-burn engine; especially the improvement of the combustion, the development of an engine management system and the achievement of vehicle test results.

However, the lean burn has high requirements on the design and manufacture of the injector. If the arrangement is unreasonable and the manufacturing precision is not up to the requirement, the rigidity of the cylinder head is insufficient which even causes leaking. Therefore, these technical problems have limited the application of lean combustion technology to a certain extent.

In summary, the application of the above technologies contributes to the improvement of fuel economy of gasoline engines, and some technologies have been successfully applied on engines, but each method has its advantages and disadvantages.

In recent years, the camless drive variable valve-train technology with canceled throttle have attracted much attention. This technology can realize the full flexibility of valve lift, phase and duration according to different working conditions, and effectively improve the power performance and fuel economy of the engine [14]–[17]. The camless driving mechanisms includes three types: electrohydraulic drive, electromagnetic drive and electric drive.

As early as 1996, Ford Company proposed the scheme of electro-hydraulic drive valve-train driven by hydraulic piston, and officially used the term “camless engine” for the first time [24]. In recent years, Lotus Company [14], the university of Perugia [25] and Minnesota [26] have entered into in-depth research on electro-hydraulic drive. The most typical application is Fiat’s Multiair electro-hydraulic drive variable valve-train technology. Heisner and Corxell [27] introduce that Fiat’s Multiair have greatly improved engine power and torque output, while reduce carbon dioxide emissions and

saved fuel. However, due to the need of hydraulic pump and electro-hydraulic servo valve, the system complexity is increased. In addition, the liquid medium is easy to leak and greatly affect by temperature and other problems need to be further solved.

In recent years, the electromagnetic drive valve-train has been the focus of domestic and foreign research institutions. As early as 1994, General Motors started the research on electromagnetic drive valve-train, and put forward the drive scheme of double electromagnet and double spring [28], which has been influencing the development direction of electromagnetic drive valve-train. Further research has also been carried out by FEV [29] and Valeo Company [30], the university of California [31] and Michigan [32]. However, the large size of the prototype, the contradiction between the limit installation space and the driving force, the accurate control of the valve movement, the energy consumption of the system and other problems need to be further solved.

Compare with the electro-hydraulic drive valve-train and electric drive valve-train, the electromagnetic drive valve-train has the advantages of quick response, simple structure and high repeatability. Electromagnetic drive valve-train is an ideal camless drive valve-train and has a broad application prospect.

Therefore, this paper designs a new type of electromagnetic driving valve-train to replace the traditional cam based on the moving-coil ELA by conducting in-depth research on the camless variable valve-train technology. The main contents of the paper are as follows:

- (1) Introduce the principle of the EMVT and design a moving coil electromagnetic linear actuator for modifying engine valve-train;
- (2) Research and analyze the method of improving engine charging efficiency under different working conditions, and plan the valve movement trajectory;
- (3) Firstly, the genetic algorithm is adopted to optimize valve motion trajectory under commonly working conditions. Secondly, the improved neural network algorithm is used to choose the corresponding valve operation mode under different working conditions. At last, the simulation and experiment are carried out by comparing with the prototype in charging efficiency so as to verify the effectiveness of the engine performance improvement using the EMVT.

The program proposed by the paper can real-time plan the motion trajectory of the actuator (valve) according to different engine operating conditions, and always keep the engine valve-train in the optimal operation mode to further improve the charging efficiency and reduce carbon dioxide emissions.

II. ELECTROMAGNETIC VALVE-TRAIN

A. THE SYSTEM DESIGN OF ELECTROMAGNETIC VALVE-TRAIN

In the electromagnetic valve-train, the energy is provided by the battery, and the electric energy is converted into the kinetic energy of the valve movement by the electromagnetic

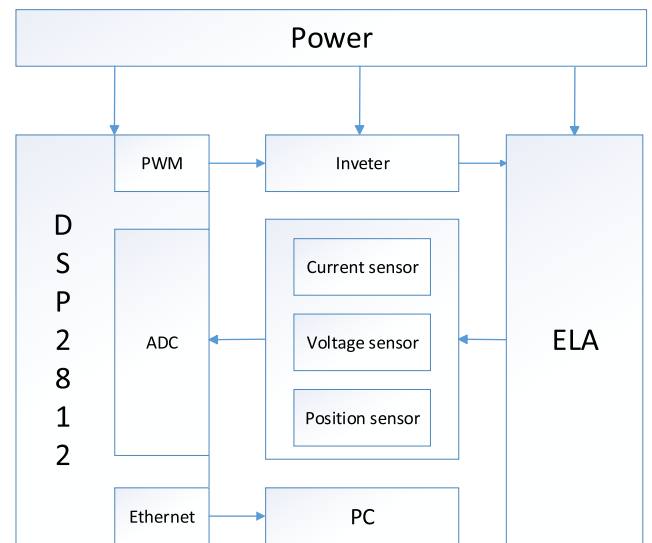


FIGURE 2. The system scheme of EMVT.

linear actuator (ELA). Through the control of ELA, the valve operation parameters such as valve timing, valve lift and valve opening duration can be controlled. Therefore, according to the operation mechanism analysis of the electromagnetic valve-train system, the electromagnetic drive valve system should be mainly composed of electromagnetic linear actuator, electronic control unit, power drive module and signal feedback module, as shown in Fig. 2.

B. THE PRINCIPLE OF ELECTROMAGNETIC LINEAR ACTUATOR

The EMVT adopted the ELA developed by our research group. Liu and Chang [33], [34] introduced that its structure mainly consisted of permanent magnet, inner yoke, outer yoke, electromagnetic coil and valve. The structure was shown in Fig. 3. The moving coil (electromagnetic coil) was located in the magnetic field between the inner and outer yokes (permanent magnets) and was rigidly connected to the driven valve. When the electromagnetic coil was energized, the axial electromagnetic force directly drove the valve movement [35]–[38].

The ELA was a complex system of machinery, circuit and magnetic circuit coupling each other. As shown in Fig. 4.

In the electromagnetic linear actuator, the inner and external yokes of actuator was made of No.08 steel with higher magnetic permeability, less coercive force and saturation magnetization. The permanent magnet adopted a high-performance permanent magnet material-NdFeB, which had high residual magnetic flux density and coercive force. The permanent magnets were arranged in an array of eight magnetic tile splicing schemes. The coil was wound on the specific shape framework with equal length opposite direction and cascade. The coil framework was made of epoxy resin material with high mechanical strength, non-conductivity, good machinability and low density.

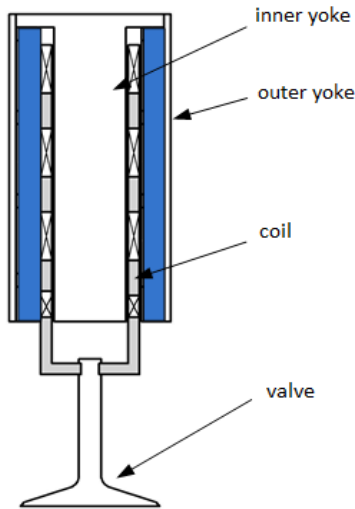


FIGURE 3. The structure of the valve-train based on the ELA.

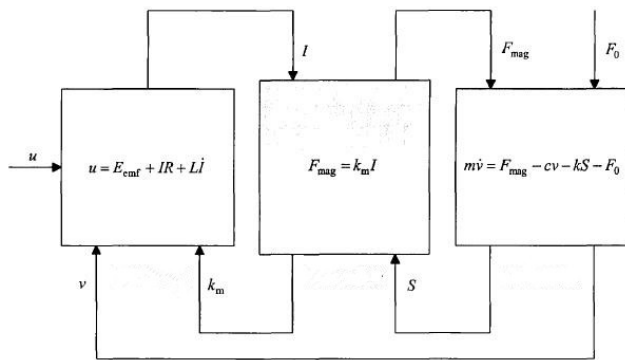


FIGURE 4. Subsystem coupling relationship in ELA.

After the optimization design, the structure size and parameters of design were shown in Table 1:

The actuator had the advantages of small motion inertia and compact structure. It could flexibly control valve lift, valve opening phase and valve opening transition time by controlling the current, thus laid down the basis of the optimal valve operating mode for further improving the performance of the engine.

C. THE DESIGN OF HARDWARE AND SOFTWARE FOR CONTROL SYSTEM OF EMVT

1) THE STRUCTURE AND HARDWARE OF CONTROL SYSTEM
The movement of the engine valve required fast response satisfying the requirement of high speed, as well as high control accuracy and robustness. Therefore, more advanced and complex control algorithm should be adopted, and put forward high requirements for the design of the control system. In this paper, DSP TMS320F2812 was taken as the core processor of the control system for its superior computing power and abundant peripheral equipment.

In Fig.2, the power inveter circuit adopts H-type fully controlled switching power element for pulse width modulation (PWM) control method. The voltage, current and

TABLE 1. Size and parameters of electromagnetic linear actuator.

Parameter	Quantity	Value
r	Radius	18 mm
h	Height	78 mm
V	Volume	79.4 cm ³
m	Moving mass	94.6 g
R	Resistance	1.3 Ω
L	Inductance	0.94 mH
S	Displacement	8 mm
F _m	Maximum electromagnetic force	360 N
a _m	Maximum acceleration	3806 m/s ²
I _m	Maximum current	30.4 A
U	Driving voltage	42 V
K _e	Back electromotive force constant	12 V · s/m
K _m	Force constant	12 N/A
c	Damping coefficient	2 N/(m · s-1)

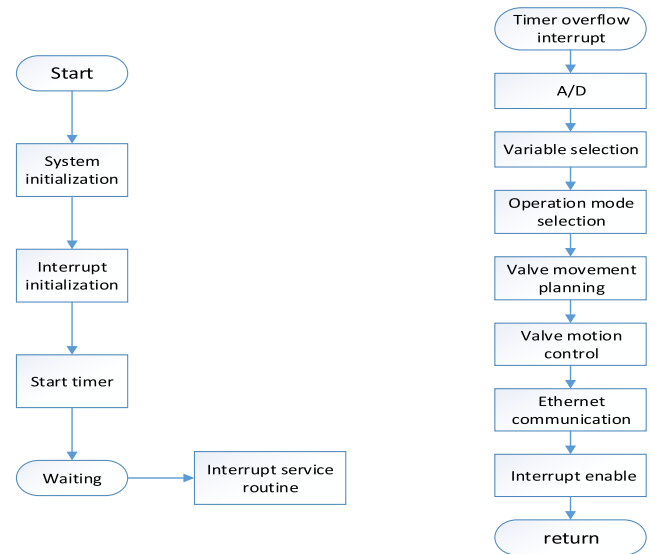


FIGURE 5. Software framework of control system.

displacement signals of the EMVT are respectively monitored by closed-loop Hall current sensor (TBC10SY), voltage sensor (SMIV±50DCE) and magnetoresistive linear displacement sensors. Through the control of the PWM waveform, the voltage across the EMVT is adjusted to realize the current control of the electromagnetic coil, and achieves the control of the valve motion law.

2) THE SOFTWARE DESIGN OF CONTROL SYSTEM

The control system software of EMVT was mainly composed of main program and interrupt service program. The software framework of the control system was shown in Fig.5.

D. FEASIBILITY ANALYSIS OF EMVT BASED ON MOTION CONTROL OF ELA

In the EMVT, since the engine valve was rigidly connected to the ELA, the motion state of the valve was closely related to

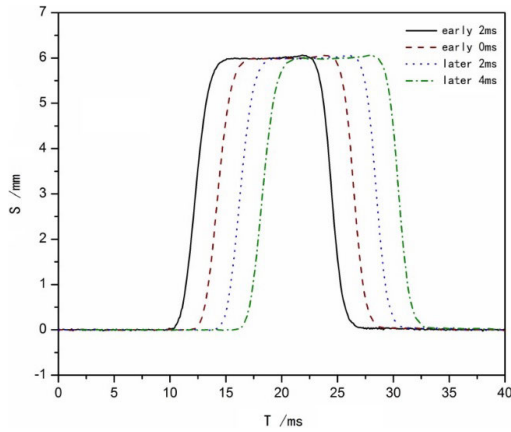


FIGURE 6. Achieving different valve timing requirements of the actuator.

the ELA. Therefore, we could continuously adjust the valve lift, phase and duration in real time by adjusting the motion parameters and state of the ELA.

1) REALIZING VARIABLE VALVE TIMING

The valve timing was achieved by adjusting the motion parameters of actuator to change the valve opening and closing timing (advance and delay). The experiment results of the actuator were shown in Fig.6. In addition, the valve opening duration could be varied by changing the timing of valve opening and closing.

2) REALIZING VARIABLE MAXIMUM LIFT

The adjustment of the valve lift was realized by changing the target position of the actuator. The experimental results were shown in Fig.7. The target valve lift was 4 mm, 6 mm and 8 mm with the transition time of 3.5 ms. It was also possible to achieve any continuously adjustable valve lift between 0 and 8 mm.

3) REALIZING VARIABLE TRANSITION TIME

Flexible adjustment of the transition time of the valve opening and closing process was realized by changing the parameter of the actuator state feedback controller. The experimental results were shown in Fig.8. Since the transition time of valve opening and closing was affected by the maximum opening lift of the valve and the performance of the actuator itself, the maximum response time of the ELA was 3ms when the maximum lift was 8mm, which can satisfy the engine requirements at 6000 r/min (10 ms for one cycle and 3 ms for transition time).

4) THE TEST OF RELIABILITY

ELA was easily affected by the external working environment, so it is necessary to research the reliability of the mechanism. The experimental results were shown in Fig.9. The transition time of valve opening/closing was 3ms, the maximum lift was 8mm, the valve runs 1000 times per minute, the cycle period was 60ms, and the sampling was 200 times.

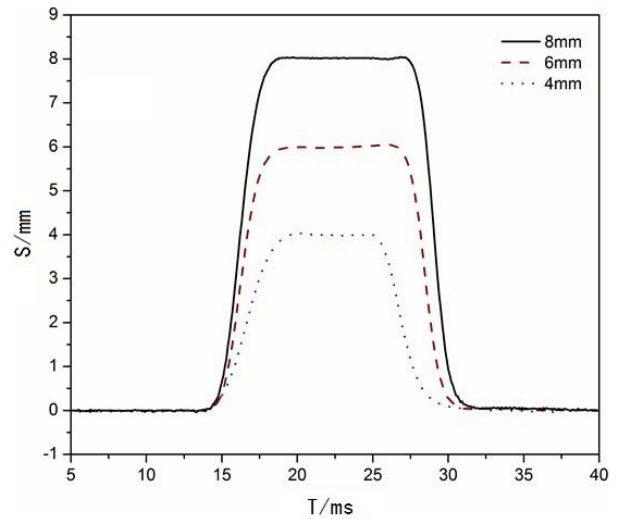


FIGURE 7. Achieving different valve opening requirements of the actuator.

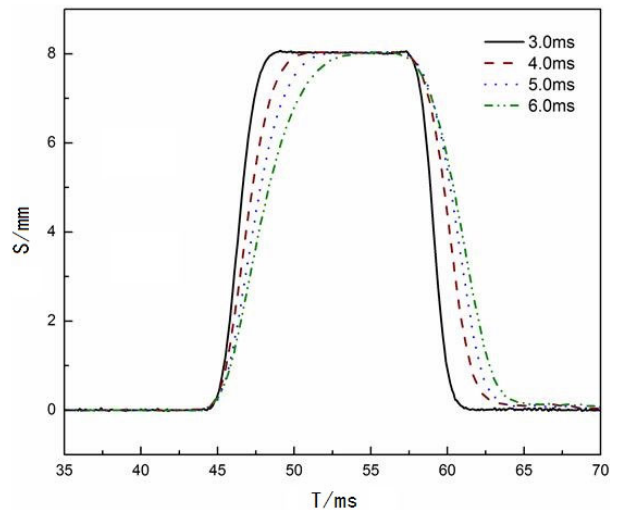


FIGURE 8. Achieving different valve over-time requirements of the actuator.

The experimental results showed that the ELA had good controllability and reliability, which could meet the needs of research work and provide guarantee for the next modification work.

5) POWER CONSUMPTION OF ELA

The motion law of the EMVT was achieved by controlling the electromagnetic force through adjusting the magnitude and direction of the current in the ELA. The power consumption of the EMVT was mainly derived from the ELA, which was closely related to the motion law of the actuator. The energy loss consisted of the conversion from electric energy to magnetic energy and the conversion from magnetic field energy to mechanical energy, which included: copper consumption, iron loss, mechanical loss. According to the conservation of energy, the energy loss would come from the electrical energy input, so the total power consumption of the EMVT could be

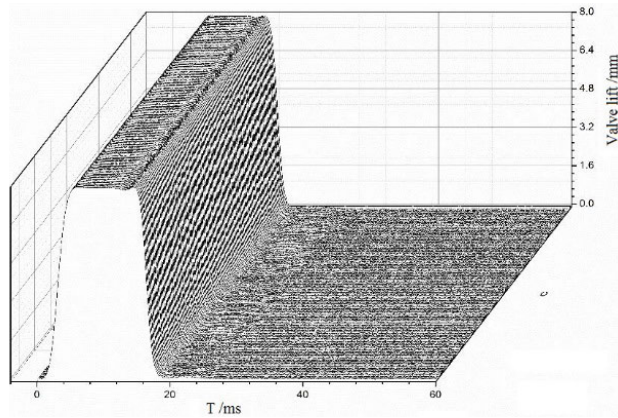


FIGURE 9. The repeatability test of ELA.

calculated by Formula (1):

$$P_{in} = UI \tag{1}$$

From the experimental results in Fig.10, we got the following analysis and inference as follows:

(1) Analysis of experimental results: The main reason of power loss was the largest current change in the opening and closing phase, but the holding current in the maximum displacement phase (valve holding period) was small.

Because of the throttle was eliminated in the EMVT, the engine load was mainly adjusted by the intake valve closing time. Therefore, it could be inferred that the engine did not bring about significant changes in valve power consumption when the engine load was adjusted by the valve duration.

(2) Analysis of experimental results: In the case of the same transition time, the larger the actuator displacement, the greater the inertial force needed to be overcome, the larger the drive current, and the greater the power lost.

It was inferred that selecting the lower valve maximum opening lift could not only assist in the adjustment of the engine charge, but also save the driving power consumption of the EMVT, which was beneficial to improving the fuel economy of the engine.

(3) Analysis of experimental results: In the case of the same displacement, the shorter the response time of the actuator, the greater the inertia force needed to be overcome, the larger the drive current and the greater the power lost.

It was inferred that selecting a slower valve transition time could save the power consumption.

Through the above analysis, the driving power consumption of the EMVT differed depending on the movement state of the valve. Therefore, it was necessary to combine the driving power consumption of the ELA with the pumping loss of the engine to reasonably plan the valve trajectory under different working conditions to improve the charging efficiency of the engine, and at the same time reduced the driving power consumption and pumping loss as much as possible to improve fuel economy.

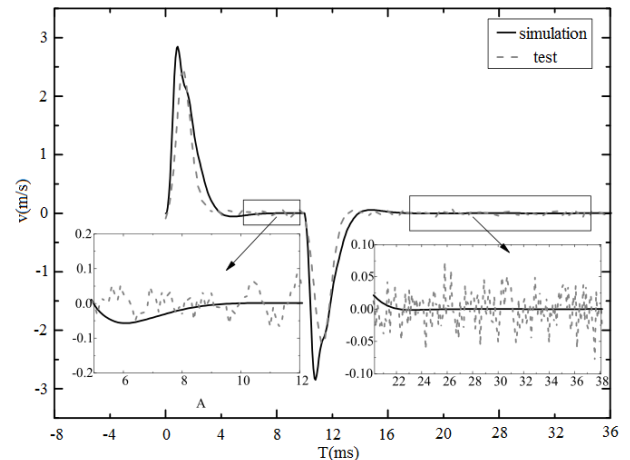
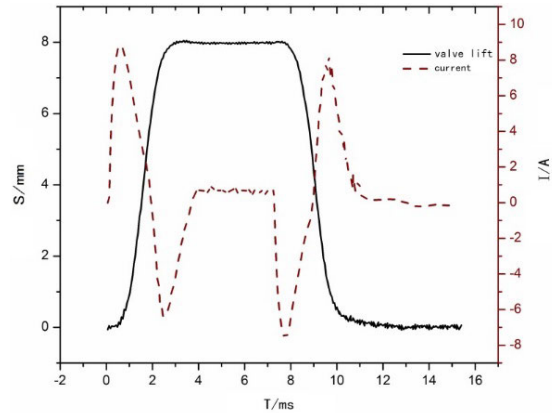


FIGURE 10. Current, displacement and velocity of the actuator.

E. MODIFICATION SCHEME OF EMVT

The four-cylinder engine prototype was used in the experiment, which adopted double cam top type (DOHC), 4-cylinder, 16-valve, naturally aspirated. The parameters were shown in Table 2. The original cam mechanism was replaced by the EMVT, as shown in Fig. 11 and Fig. 12.

III. THE ANALYSIS OF VARIABLE VALVE TO IMPROVE ENGINE CHARGING EFFICIENCY

A. VARIABLE VALVE PHASE BOOSTING CHARGING EFFICIENCY

1) THE EFFECT OF VALVE CLOSING AND OPENING PHASE ON CHARGING EFFICIENCY

The cam profile design of the conventional cam type valve-train preferentially guaranteed the power performance at high speed. In the low speed, as the inflation speed decreases, the excessive intake closing phase caused a part of the air to flow back to the intake pipe, which caused the decline of charging efficiency. Therefore, the variable valve technology could flexibly adjusted the closing phase with the change of the rotational speed to improve the charging efficiency. As shown in Fig.13, a smaller closing angle can increase the charging efficiency at the lower speed.

TABLE 2. The parameters of engine.

Parameter	Value
Number of cylinders	4
Number of valves	16
Compression ratio	10.5:1
Intake Type	Naturally aspirated
Displacement /L	1.8
Nominal power /kW	96.5
Nominal speed /(r.min ⁻¹)	6000

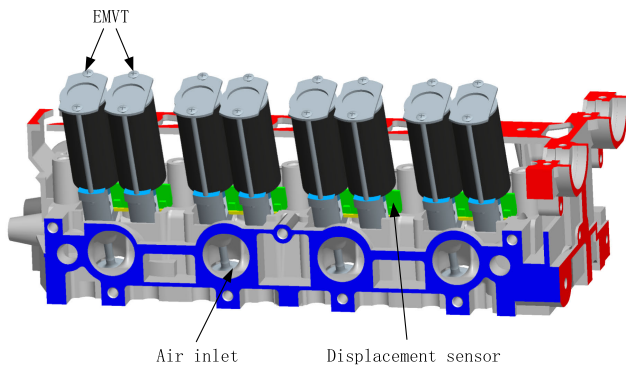


FIGURE 11. The design drawing of EMVT modification.

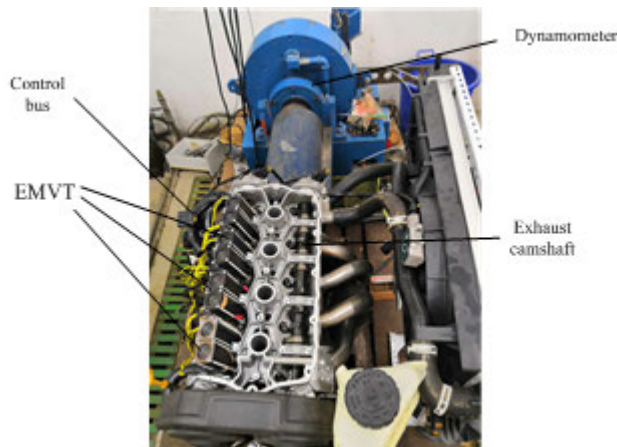


FIGURE 12. The physical picture of the EMVT modification.

Regarding to the valve opening phase, there were two types: early intake valve opening (EIVO) and late intake valve opening (LIVO). The valve opening (IVO) phase had a direct effect on the amount of residual exhaust gas and the duration of the charge, that is, too early opening valve would cause excessive residual exhaust gas volume, and too late opening valve would cause a decrease in charging efficiency. Therefore, it could be inferred that under different speed conditions, there was a set of theoretically optimal valve timings to maximize engine charging efficiency.

2) UNDER LOW SPEED CONDITIONS

Under the condition of low speed about 1000r/min, the engine had lower inflation speed and less inflation inertia.

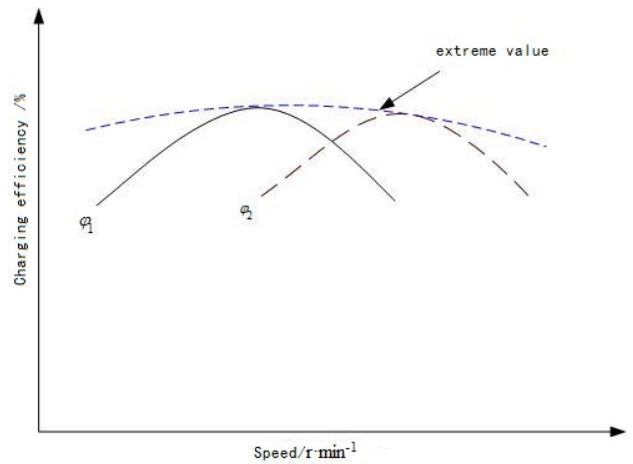


FIGURE 13. Charging efficiency of different intake valve closing angles.

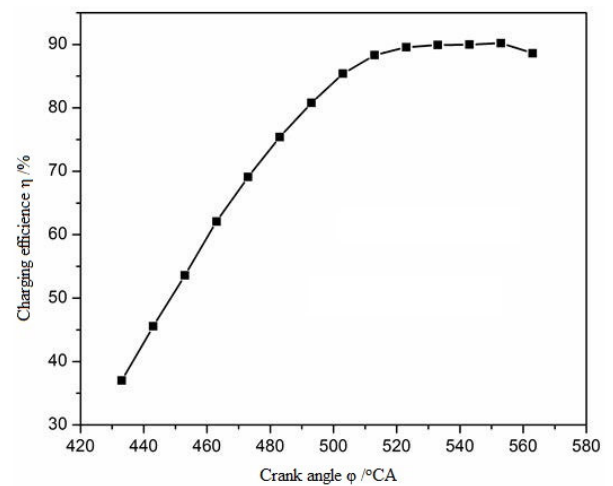


FIGURE 14. Charging efficiency changes with the IVC under low speed conditions.

The experimental results of charging efficiency with the change of valve closing and opening phase were shown in Fig. 14.

The engine charging efficiency varied linearly in the range of 35%~85% (430° ~520°ca) with the IVC, but as the piston run near the bottom dead center of the engine, the piston speed was very low and the cylinder volume changed very small, at this time the inflating volume closed to saturation which did not change significantly with the phase of IVC.

It could be obtained from the experimental Fig. 15 that as the IVO advancing, the inflating volume of the engine decreases and the charging efficiency decreases. This was because a certain amount of exhaust gas enters the intake pipe, and the amount of fresh air in the cylinder was reduced. Therefore, it could be inferred that LIVO would increase the inflation flow rate, and the inflation inertia would increase the intake inflating volume to improve the inflation efficiency.

3) UNDER HIGH SPEED CONDITIONS

The experimental results of the variation of the inflation flow with IVO at 6000 r/min of the engine were shown in Fig. 16.

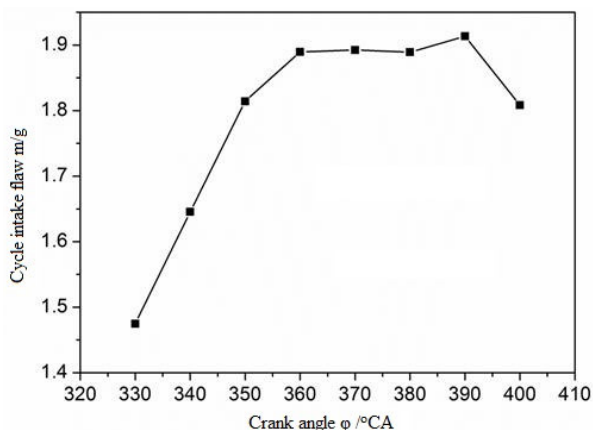


FIGURE 15. The variation of the inflating volume with IVO under low-speed conditions.

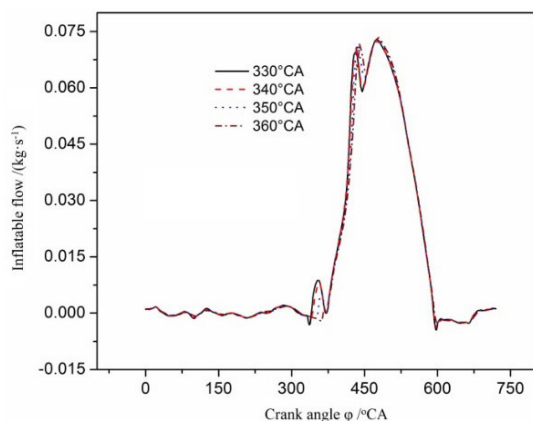


FIGURE 16. Different inflation flow with IVO under high speed.

It could be seen from Fig.16 that the inflation flow could be increased by EIVO, in order to ensure the enough time-area value, and improve the charging efficiency at the high engine speed. However, it should be noted that early intake valve opening may interfere with the piston movement. Therefore, we first chose to open at 4mm, then opened at 8mm.

B. VARIABLE VALVE LIFT FOR IMPROVED EFFICIENCY

1) THE EFFECT OF VALVE LIFT ON CHARGING EFFICIENCY

At present, there are two kinds of statements about the valve lift when the intake valve phase is constant. One is the larger maximum opening lift of the valve, the large time-area value is, the smaller the air passage resistance is, and the better the airflow passing ability is. The other is that reducing the maximum opening lift can throttle down, which can increase inflatable flow by using the inertia of the intake air, and is also beneficial to improve the combustion performance of the engine. In order to identify the two viewpoints applicable to the engine speed conditions, the effect of the maximum lift of the valve on the charging efficiency is discussed. During the experiment, the low, medium and high engine

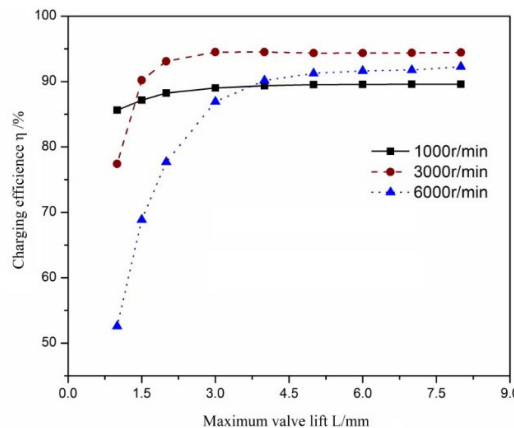


FIGURE 17. Inflation efficiency of valve lift at different speeds.

speeds (1000r/min, 3000r/min and 6000r/min) were taken for analysis. The experimental results were shown in Fig. 17.

Through the experimental results, the following conclusions could be drawn as follow:

1) In the low engine operating condition (1000 r/min), as the valve lift increases, the charging efficiency of engine gradually increased, but when the lift was more than 5 mm, the charging efficiency tended to be slow or even unchanged. The intake efficiency of the valve with a maximum opening lift of 1 mm was only 4.4% lower than that of 8 mm, which indicated that the charging efficiency was less affected by the change of the valve opening lift at the low speed.

2) In the high engine speed condition (6000r/min), in order to increase the charging efficiency of engine, it was necessary to increase the valve lift to ensure the enough time-area value. The charging efficiency of 8mm increased 15.7% compared with that of 2mm, which indicated that the maximum lift of the valve had a great influence on the charging efficiency under the high engine speed condition. Therefore, in order to meet the needs of charging efficiency at high engine speeds, a larger valve lift was required.

3) When the engine was in medium speed (3000r/min), the peak of the charging efficiency was significantly higher than that of the low speed and high speed, which had higher charging efficiency. This indicated that the maximum lift of the valve was more sensitive to the charging efficiency. After 6mm lift, the charging efficiency tended to be stable and was close to saturation.

2) INFLUENCE OF VALVE LIFT VARIATION ON PUMPING LOSS AND POWER CONSUMPTION

Through the above analysis of the charging efficiency under different working conditions, it could be known that within a large lift range (6mm~8mm), the charging efficiency was not much different. However, when the valve lift was changing, the driving power consumption of the ELA and the pumping loss of the engine were different. If it is beneficial to the improvement of the engine power or not, further comprehensive analysis should be carried out. Therefore, the pumping

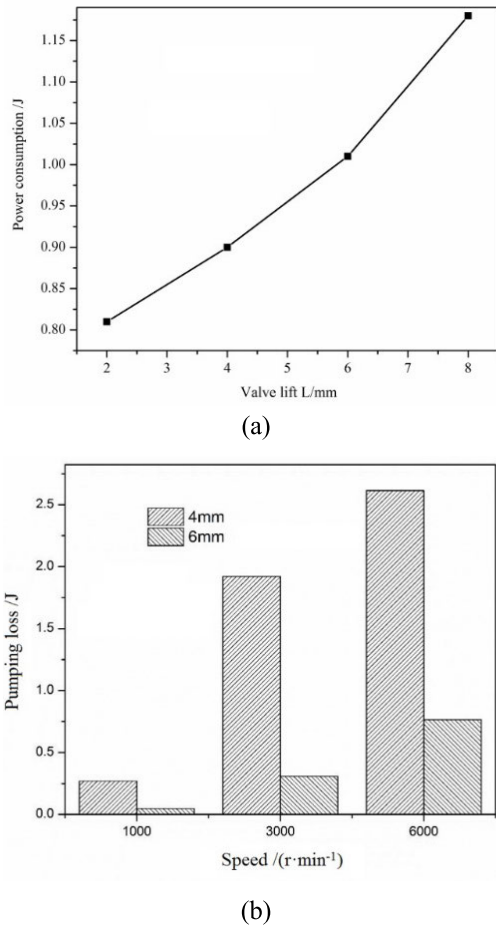


FIGURE 18. The power consumption (a) and pumping loss (b) under different valve lifts.

loss of the engine and the power consumption of the ELA were respectively compared under the maximum lift of 2mm, 4mm, 6mm and 8mm, the results were shown in Fig. 18.

It could be seen from the experimental results in the Figure that the pumping loss of engine increased as the engine speed increases. At the same speed, increasing the maximum lift of the valve could reduce pumping losses. But at the same time as the lift increases, the actuator power consumption will increase.

Based on the above analysis, we can get the following results:

(1) Under low speed conditions(1000r/min), the charging efficiency was not significantly reduced when the smaller lift was 4mm, but the reduction of power consumption was much larger than the pumping loss, which could reduce the power consumption 27.5%;

(2) Under medium speed conditions (3000r/min), the increasing amount of pumping loss of 6mm compared with 8mm was equivalent to the power consumption saved by the EMVT, but the flow rate of the working fluid increased, so choosing 6mm was better than 8mm;

(3) Under high speed conditions (6000r/min), the smaller valve lift could not ensure enough air volume, and the saved

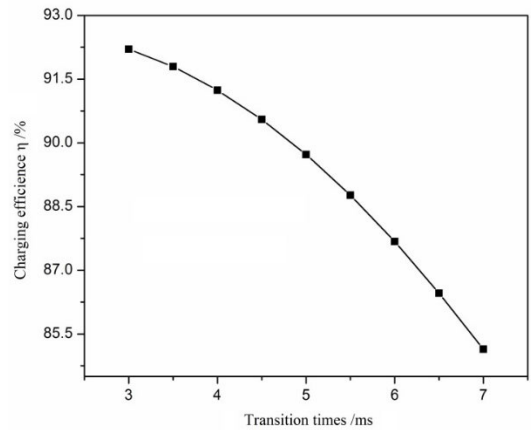


FIGURE 19. The charging efficiency at different valve transition times.

power consumption by the valve-train was insufficient to compensate for the increase of pumping loss, which was not conducive to improve the power performance, so you needed to choose a larger valve lift.

C. VARIABLE TRANSITION TIME FOR IMPROVING PUMPING EFFICIENCY

The transition time of the valve opening and closing process could be adjusted by the control system. The charging efficiency was different under different valve transition times. The experimental results were shown in Fig.19.

It could be seen from the Fig.19 that the charging efficiency of the engine gradually decreased as the transition time increases, up to 92.2% when the valve transition time was 3 ms. At low and medium speed conditions, the transition time of the EMVT was sufficient to meet the operational requirements. However, under high-speed conditions, transition time would affect the valve lift, for example, the engine was 6000r/min as shown in Fig.20.

It could be seen from the Fig.20 that due to the constraint of the cycle time, after the transition time was greater than 3.5ms, the valve would be forced to close and the maximum opening lift was less than 8mm.

In addition, the different of transition time would also cause the different change of the pumping loss of the engine and the power consumption of the valve-train. Therefore, the selection of the best transition time under different working conditions should not only consider from the aspect of charging efficiency, but also the comprehensive aspects of power consumption and pumping loss. The experimental results were shown in Fig.21.

With the increase of valve transition time, the driving power consumption and pumping loss of the EMVT were oppositely changing, the valve drive power consumption was gradually reducing, and the pumping loss was gradually increasing.

Based on the above analysis, in the case of high speed condition, selecting a smaller transition time was more advantageous to ensure the improvement of engine power

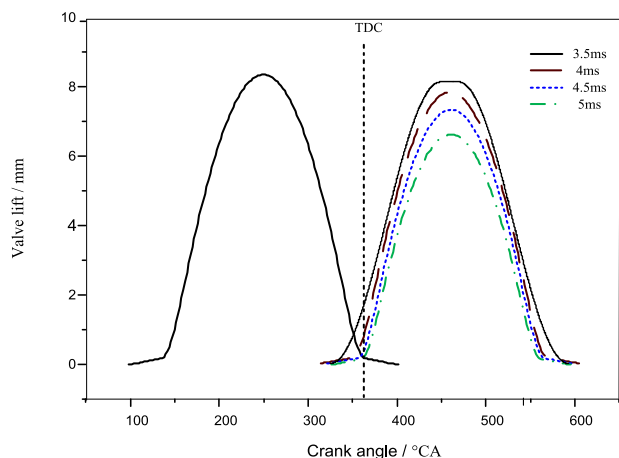


FIGURE 20. Valve lift curve under different transition times at 6000r/min.

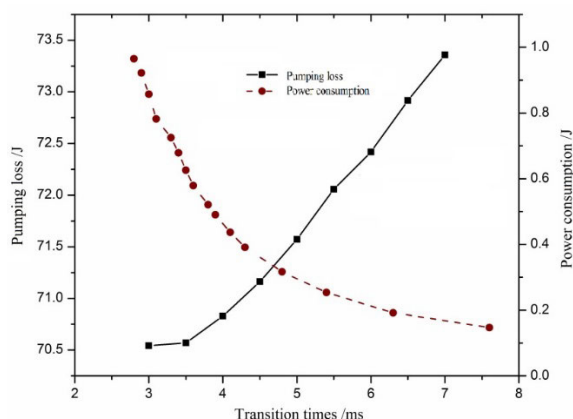


FIGURE 21. Pumping loss and power consumption with different transition times.

performance; under lower engine speed conditions, selecting a longer transition time would make the engine more energy-saving.

D. DIFFERENT VALVE OPERATING MODE FOR IMPROVING CHARGING EFFICIENCY

Since the single intake valve operating mode could save drive power consumption compared with the dual intake valve operating mode. Therefore, in the low-speed condition, if the single intake valve operating mode could ensure the charging efficiency and the increase of the pumping loss could be compensated by the reduction of the EMVT driving power consumption, priority was given to the single valve operating mode. The experimental results of the charging efficiency of the different valve operating modes were shown in Fig.22.

We could conclude the results from the Fig.22 as follows:

- (1) In the speed region of 1000~2500r/min, comprehensive analysis of the pumping loss and driving power consumption, the single valve working mode should be adopted.
- (2) In the speed region of 2500~3000r/min, although the increase of pumping loss was slightly larger than the driving power consumption saved by the valve-train, but the single

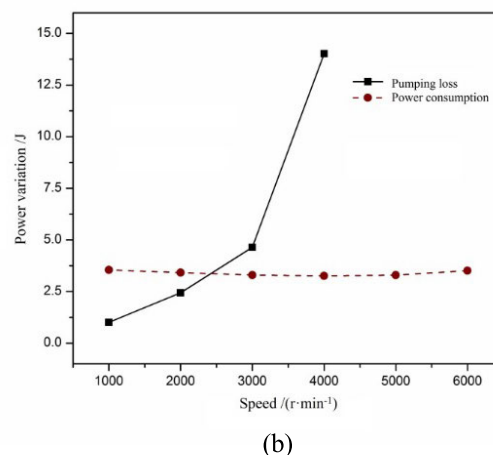
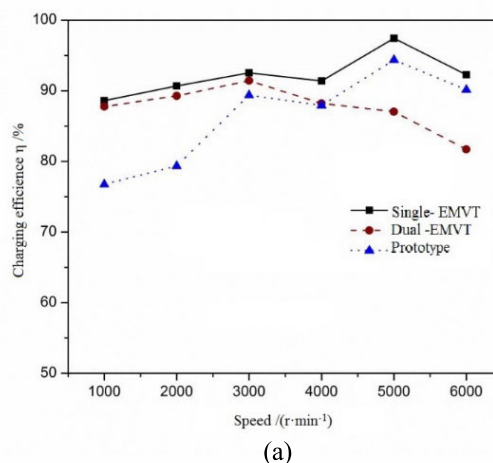


FIGURE 22. Charging efficiency (a), single valve pumping loss and power consumption (b) in different valve operating modes.

valve operating mode could greatly improve the intake air flow rate and improve the quality of fuel and air mixing. Priority was given to the single valve operating mode;

- (3)When the speed was higher than 3000r/min, the charging efficiency was decreased and the pumping loss was also increased rapidly. The saved power consumption was not enough to compensate for this increment of the pumping loss. The dual valve operating mode should be adopted.

IV. OPTIMIZATION OF THE VALVE MOTION TRAJECTORY PLANNING AND OPERATION MODE OF EMVT

A. SET VALVE MOVEMENT PARAMETERS UNDER THE EXTREME CONDITION OF CHARGING EFFICIENCY

In the previous research, due to the constraints of the existing ELA performance (The fastest response time of 3ms) and engine parameters (The maximum lift of 8mm), in order to achieve the maximum charging efficiency, we further optimized the valve operating parameters through simulation software to explore the limit value of the charging efficiency. Set the valve transition time to 2ms and the valve lift to 10mm. The simulation results are shown in Fig. 23.

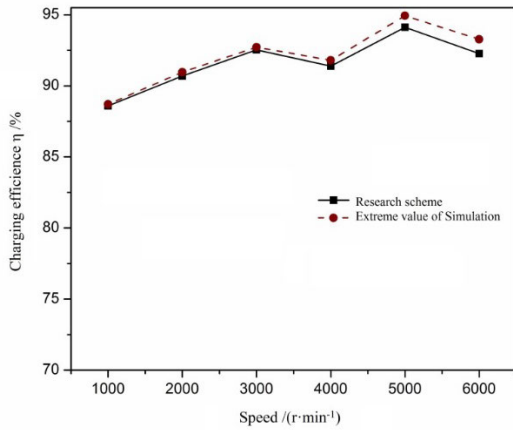


FIGURE 23. Simulation of inflation efficiency limit.

As can be seen from Fig.23, the extreme value of the charging efficiency obtained by simulation was not much different from the existing scheme when the engine speed was less than 4000 r/min, but the extreme value was slightly increased compare with the existing scheme after the engine speed was higher than 4000r/min, which was increased by about 1.2% at 6000r/min. Therefore, the simulation results could verify that the charging efficiency of our research scheme in this paper by setting value transition time of 3ms and maximum valve lift of 8mm was already very high. At the same time, the ELA designed by our research team could meet the requirements of engine valve movement.

B. OPTIMIZATION OF THE VALVE MOTION TRAJECTORY PLANNING BASED ON GENETIC ALGORITHM

Through the previous analysis, according to the fully flexible characteristics of the electromagnetic variable valve, the operating parameters of valve could be further optimized to obtain the optimal valve trajectory under different working conditions, and improved the power performance, fuel economy, and emission performance.

Due to the complicated working conditions of the engine, the motion trajectory of the valve varies with the different working conditions, and the amount of calculation was very large. Therefore, this paper adopted genetic algorithm to optimize the trajectory [39]–[43]. The genetic algorithm was first proposed by Professor J. Holland in 1975. Its main advantages are to realize simultaneous search for multiple points, reduce the possibility of convergence to local solutions in the iterative process, and search for complex spaces with multiple peaks. The characteristic of genetic algorithm is directly operating on the structural object, which is not limited by the derivative and the continuity of the function. Adopting the probabilistic optimization method can automatically acquire and guide the optimized search space and adaptively adjust the search direction without determining the rules. This is very suitable for the optimization of the valve motion trajectory of the EMVT researched in this paper.

In the optimization of the valve trajectory, the following variables were set: valve opening time φ_1 , valve closing

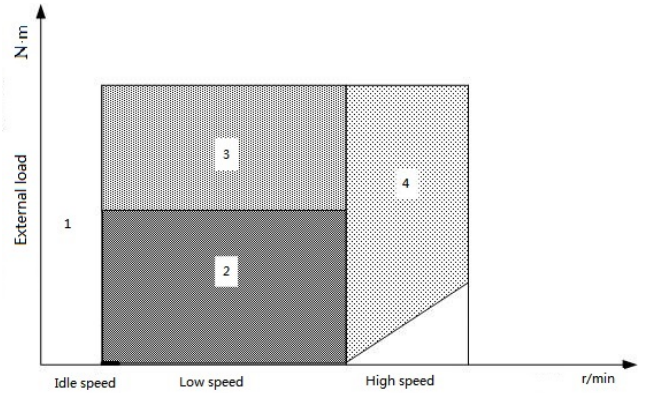


FIGURE 24. The optimal scheme of valve motion trajectory under common working conditions.

moment φ_2 , valve lift S_1 , the number of valves per cylinder S_2 , valve transition time S_3 . The charging efficiency is set to the optimization target. Because the EMVT realized continuous adjustment of the valve timing, φ_1, φ_2 were set to continuous variable, and the valve lift S_1 and the transition time S_3 were set to discrete values and the appropriate gradient was selected.

1) Setting variables:

Continuous variables: φ_1, φ_2 ;

Discrete variables: $S_1 = 2\text{ mm}, 4\text{ mm}, 6\text{ mm}, 8\text{ mm}, \varphi_2 = 1, 2, S_3 = 3\text{ ms}, 4\text{ ms}, 5\text{ ms}$;

2) Setting constraints:

$$\begin{cases} -30^\circ CA \leq \Delta\varphi_1 \leq 10^\circ CA \\ 0 \leq \Delta\varphi_2 \leq 10^\circ CA \end{cases} \quad (2)$$

3) Setting optimization goals:

The minimum charging efficiency η_v was set to the optimization goal. The expression was:

$$\min = F(X) \quad (3)$$

$$F(X) = \eta_v(\varphi_1, \varphi_2, S_1, S_2, S_3) \quad (4)$$

Through the optimization of the valve operating parameters of the engine under various working conditions, the most suitable working range of the valve working mode was obtained, and the optimal valve trajectory under different working conditions was gained as shown in Figure 24.

According to the performance requirements of the engine under different working conditions, the optimal operation parameters of the valve were calculated with the objective of optimal inflation efficiency, and the optimal motion trajectory planning of the valve under common working conditions were shown in Fig. 24-28:

The planning scheme for optimal valve trajectory under different working conditions was listed as follows:

(1) Idle condition: LIVO, small lift (3mm), single valve. The trajectory was as shown in Fig.25.

(2) Low-speed and low-load working conditions: EIVO, small lift(4mm), single valve. The trajectory was as shown in Fig.26.

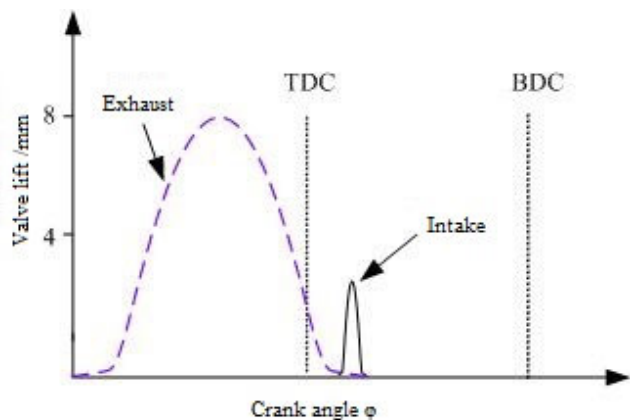


FIGURE 25. Valve trajectory under idle condition.

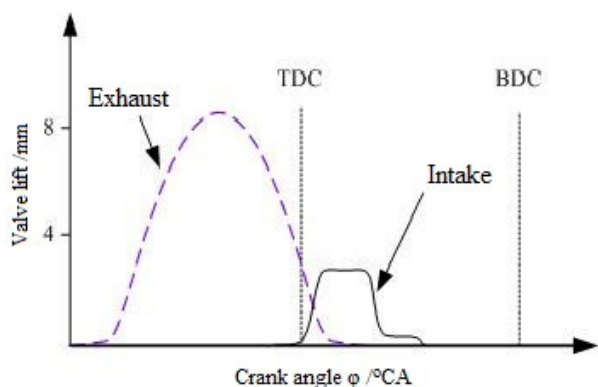


FIGURE 26. Valve trajectory at low-speed and low-load conditions.

(3) Low-speed and high-load working conditions: EIVO, the large lift (8mm), the double valve. The trajectory was as shown in Fig.27.

(4) High speed working condition: EIVO, LIVC, large lift (8mm), double valve, transition time(3ms).In order to avoid the interference of valve movement and piston motion, the intake valve opened a small lift (4mm) in advance, as shown in Fig. 28.

Through the above analysis, the four valve trajectories of the engine under common working conditions were obtained, but the running state of the engine changes in real time. So we could select the corresponding optimal operating mode from the range of all working conditions based on the optimal trajectory planning under common operating conditions according to engine power, load and speed, etc.

C. OPTIMAL SELECTION OF OPERATING MODE BASED ON IMPROVED BP NEURAL NETWORK ALGORITHM

Because of its simple structure and strong plasticity, BP neural network was widely used in the fields of function fitting, parameter identification and classification. The fault monitoring and diagnosis of ELA was a classic parameter identification and classification problem. Therefore, the BP neural network was chosen as the model basis for fault diagnosis in this paper.

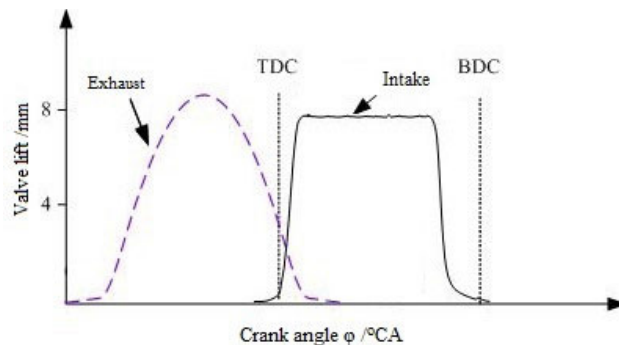


FIGURE 27. Valve trajectory under low-speed and high-load conditions.

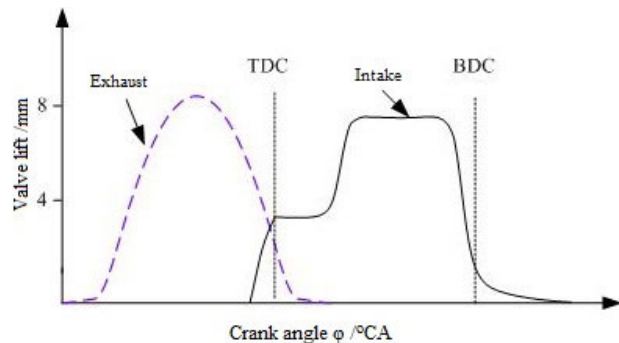


FIGURE 28. Valve trajectory at high speeds.

In the model of the BP neural network, the number of neurons in the input layer and the output layer of the neural network is determined, and the number of neurons which determines the classification ability of the network in the hidden layer is uncertain. Therefore, the correct selection of the number of neurons in the hidden layer is crucial for improving the network recognition performance. In the current research on the neural network, almost all the neurons in the hidden layer were determined according to the experimental and the empirical formula. Therefore, in order to realize real-time optimization of BP neural network structure and improve the learning speed of model training, this paper proposed Gray Relational Analysis method based on the pre-learning of BP neural network to dynamically adjust the number of neurons in the hidden layer [44]–[48].

Gray Relational Analysis (GRA), based on the mathematical statistics, finds the data (the amount of mapping) that reflects the behavior characteristics and predicts the development trend of the system through the GRA of the behavioral feature data and related factor data. The GRA method is especially suitable for small and irregular samples, which is very consistent with the characteristics of actuator fault diagnosis. The core idea of the GRA method is to judge the relationship of the sequence according to the similarity of the geometrical shapes between the sequence curves (grey correlation degree). The closer the curves of the two sequences, the larger correlation degree of the corresponding sequence [49], [50].

Optimizing the calculation parameters of the BP neural network model based on Gray Relational Analysis was as follows:

Given a training samples, $t = 1, 2, \dots, N$, the number of neurons in the input layer is n , and the number of neurons in the output layer is m , $j = 1, 2, \dots, m$. Only the number of neurons in the hidden layer q is the amount to be determined, $k = 1, 2, \dots, q$.

The expected output of the network is set to $y = (y_1, y_2, \dots, y_m)^T, y \in R$, Sequence $y_i = (y_i(1), y_i(2), \dots, y_i(N))$ is the expected output of the N samples corresponding to the i -th output neuron.

Step 1: First, collect the object data $X_i(t), t = 1, 2, \dots, N$. Then, according to the actual object, the behavioral characteristic sequence (reference sequence) responding system behavior characteristics and the related factor sequence (comparative sequence) affecting the system behavior are determined

Reference sequence:

$$X_0 = (X_0(1), X_0(2), \dots, X_0(n));$$

Comparison sequence:

$$X_i = (X_i(1), X_i(2), \dots, X_i(n)).$$

Step 2: Taking the expected output of the neural network as the reference sequence:

$$y = \begin{bmatrix} y_1 \\ y_2 \\ \vdots \\ y_m \end{bmatrix} = \begin{bmatrix} y_1(1) & y_1(2) & \cdots & y_1(N) \\ y_2(1) & y_2(2) & \cdots & y_2(N) \\ \vdots & \vdots & \vdots & \vdots \\ y_m(1) & y_m(2) & \cdots & y_m(N) \end{bmatrix} \quad (5)$$

Step 3: Taking the output sequence value of the k -th neuron of the hidden layer as the test sequence:

$$h_k = (h_k(1), h_k(2), \dots, h_k(N)) \quad (6)$$

Step 4: Finding the difference sequence according to formula (7) and calculating the maximum and minimum of the difference value:

$$\left\{ \begin{array}{l} \Delta_i(t) = |x_0(t) - x_i(t)| \\ \Delta_{\max} = \max_{i=1}^m \left\{ \max_{t=1}^n \{|x_0(t) - x_i(t)|\} \right\} \\ \Delta_{\min} = \min_{i=1}^m \left\{ \min_{t=1}^n \{|x_0(t) - x_i(t)|\} \right\} \end{array} \right\} \quad (7)$$

Step 5: Calculating the correlation coefficient $r_{ki}(t)$ between the output of the k -th hidden layer's node (comparison sequence) and the reference sequence according to formula (8)

$$r_{ki}(t) = r(x_k(t), x_i(t)) = \frac{\Delta_{\min}(k,i) + \rho \Delta_{\max}(k,i)}{\Delta_{ki}(t) + \rho \Delta_{\max}(k,i)} \quad (8)$$

In the formula, the resolution coefficient $\rho = 0.5$

Step 6: Calculating the correlation degree r_{ki} between the output of the k -th hidden layer's node (comparison sequence) and the reference sequence according to formula (9):

$$r_{ki} = r(x_k, x_i) = \frac{1}{n} \sum_{t=1}^n r(x_k(t), x_i(t)) \quad (9)$$

Taking $r_k = \max_{i=1}^m \{r_{ki}\}$ as the degree of correlation between the k -th hidden layer's node and the expected output of the network.

Step 7: Repeating steps from 1 to 6 to find the correlation degree r_k between all hidden layer's nodes and the expected output;

Step 8: Sort the gray correlation degree. Sort the result in step 7 to get a gray correlation sequence. If the value of correlation degree between the output of a hidden layer's node and the expected output is less than the pre-set value $\varepsilon \in (0, 1)$, the corresponding hidden layer neurons can be deleted, and the network structure will be optimized.

Step 9: Repeat steps from 1 to 8 until the value is not less than the preset. The number of hidden layer's nodes is optimal, and the BP neural network structure is optimized.

The flow chart of the improved BP neural network algorithms based on GRA was shown in Fig.29.

In the improved BP neural network fault diagnosis model, the structure of neural network was determined three layers according to the empirical formula, input nodes was set to 3(speed, load, inflating volume), hidden layer tentative nodes was set to 8, output nodes was set to 4(four common working conditions), the activation function of hidden layer chose logarithmic sigmoid function; the preset value of the correlation degree between the output of the hidden layer node and the expected output was set $\varepsilon = 0.5$.The number groups of each fault samples was set to 12. The input data needed to be normalized, and the number of hidden layer nodes was determined by Gray Relational Analysis.

The main training parameters of neural network algorithm were as follows:

```
.trainparam.max_fail = 5; % Max Confirmation Failures
.trainparam.goal = 0.001; % training target minimum error
.trainParam.epochs = 200; % training times
.trainParam.lr = 0.05; % learning rate
.trainParam.min_grad = 1e-6;% minimum performance gradient
```

The rest of the parameters used the default values of Matlab.

In addition, the actual neural output of network should be different from the ideal output, so we respectively set the threshold of operating mode to 0.2 and 0.8.When the output was equal to or more than 0.8, it was determined that the EMVT works in optimal operating mode, when the output was equal to or less than 0.2, it was determined that the EMVT works in wrong operating mode; when the output was between 0.2 and 0.8, it was determined that the EMVT works in non-optimal operating mode.

Based on the optimal trajectory planning under common working conditions, the optimal mode selections of valve under different working conditions were obtained, as shown in Fig. 30.

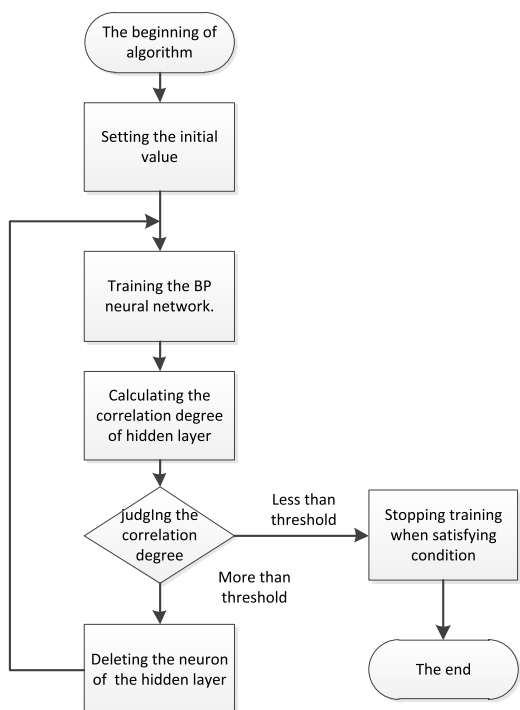


FIGURE 29. Flow chart of the improved BP neural network algorithm.

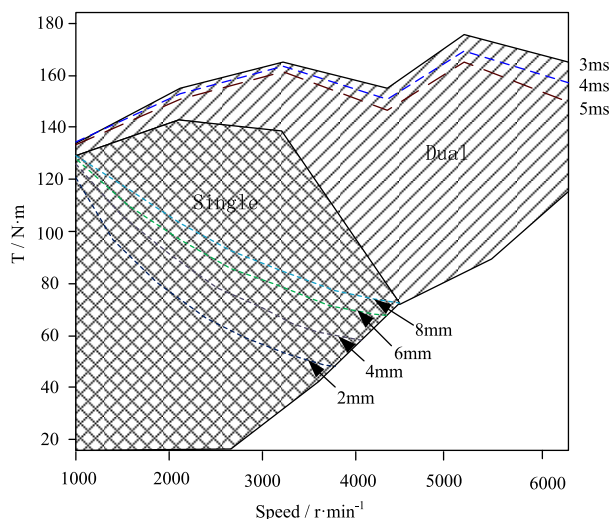


FIGURE 30. The optimal mode of valve under different working conditions.

D. COMPARISON WITH THE PROTOTYPE

The charging efficiency of engine using the optimized valve trajectory compared with the prototype at different speeds (adopted speed interval 1000r/min). The result was shown in Fig. 31.

The charging efficiency of engine using the EMVT was improved compared to the cam-driven prototype over the full speed range. The improvement in the low speed was more obvious, and the charging efficiency reached 95.6% at 5000r/min.

Through the above analysis and experiments, we could draw the following conclusions:

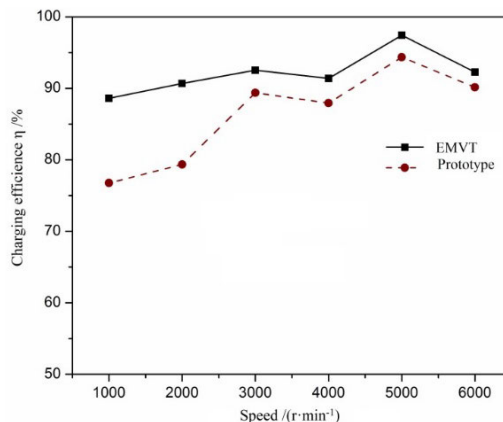


FIGURE 31. The charging efficiency at different speeds compared with the prototype.

(1) Under the low-speed working condition, adopted the single-valve and low-lift trajectory could not only improve the charging efficiency, but also reduce the pumping loss and the driving power consumption of the EMVT. Therefore, as the engine speed decreases, reducing the maximum opening lift of the valve was beneficial to improve the fuel economy.

(2) Under the high-speed working condition, when the single-valve was used, it was necessary to increase the valve lift according to the load to reduce the pumping loss caused by the throttling, and ensure the maximum charging efficiency to reduce the effective fuel consumption rate of the engine. The mode should switch to the dual valve after 4000r/min.

(3) Under the high-speed condition, the double-valve and large-lift trajectory was used to ensure the charging efficiency and reduce the pumping loss to improve the fuel economy.

V. SUMMARY

In this paper, through theoretical analysis, simulation and experimental research methods, the application of EMVT in engine intake system was deeply researched. A modified EMVT based on moving-coil ELA was designed and the feasibility analysis was put forward. Simulation result verified that the maximum response time 3ms of the ELA could meet the requirement of high-speed movement in the engine. In addition, on the premise of analyzing the performance of the engine under different working conditions, the charging efficiency of the engine was taken as the research object to re-plan the valve trajectory and accurate control of the valve movement. Through the comparison and analysis between the experimental results and the prototype, the charging efficiency had been improved in the range of full rotation speed. Especially in the low rotation speed, the improvement amplitude was more obvious up to 95.6%, which proved that the design scheme had important significance and application value for the improvement of engine performance.

REFERENCES

[1] S. Tong, X. Li, S. Liu, and J. Deng, "Effect of two-stage valve lift for fuel economy and performance on a PFI gasoline engine," SAE Tech. Paper 2014-01-2874, 2014.

- [2] B. Ashok, S. D. Ashok, and C. R. Kumar, "A review on control system architecture of a SI engine management system," *Annu. Rev. Control*, vol. 41, pp. 94–118, 2016.
- [3] B. Ashok, S. D. Ashok, and C. R. Kumar, "Trends and future perspectives of electronic throttle control system in a spark ignition engine," *Annu. Rev. Control*, vol. 44, pp. 97–115, 2017.
- [4] B. Ashok, "An integrated pedal follower and torque based approach for electronic throttle control in a motorcycle engine," *Eng. J.*, vol. 21, no. 1, pp. 63–80, 2017.
- [5] D. Petitjean, L. Bernardini, C. Middlemass, and S. M. Shahed, "Advanced gasoline engine turbocharging technology for fuel economy improvements," SAE Tech. Paper 2004-01-0988, 2004.
- [6] G. Vent, C. Enderle, N. Merdes, F. Kreitmann, and R. Weller, "The new 2.0 l turbo engine from the Mercedes-Benz 4-cylinder engine family," in *Proc. 21st Aachen Colloq. Automobile Engine Technol.*, vol. 1, 2012, pp. 137–159.
- [7] I. Watanabe, T. Kawai, K. Yonezawa, and T. Ogawa, "The new Toyota 2.0-liter inline 4-cylinder ESTEC D-4ST engine-turbocharged direct injection gasoline engine," in *Proc. Conf. 23rd Aachen Colloq. Automobile Engine Technol.*, 2014, pp. 51–78.
- [8] R. Wurms, R. Budack, J. Böhme, R. Dornhöfer, A. Eiser, and W. Hatz, "The new 2.0 L TFSI with Audi valvelift system for the Audi A4—the next generation of the Audi TFSI technology," in *Proc. 17th Aachen Colloq. Automobile Engine Technol.*, 2008, p. 1078.
- [9] C. Gray, "A review of variable engine valve timing," *SAE Trans.*, pp. 631–641, 1988.
- [10] H. Hong, G. B. Parvate-Patil, and B. Gordon, "Review and analysis of variable valve timing strategies—Eight ways to approach," *Proc. Inst. Mech. Eng., D, J. Automobile Eng.*, vol. 218, no. 10, pp. 1179–1200, 2004.
- [11] T. Hosaka and M. Hamazaki, "Development of the variable valve timing and lift (VTEC) engine for the Honda NSX," SAE Tech. Paper 910008, 1991.
- [12] D. Cleary and G. Silvas, "Unthrottled engine operation with variable intake valve lift, duration, and timing," SAE Tech. Paper 2007-01-1282, 2007.
- [13] T. Fujita, K. Onogawa, S. Kiga, Y. Mae, Y. Akasaka, and K. Tomogane, "Development of innovative variable valve event and lift (VVVEL) system," SAE Tech. Paper 2008-01-1349, 2008.
- [14] J. Allen and D. Law, "Production electro-hydraulic variable valve-train for a new generation of IC engines," SAE Tech. Paper 2002-01-1109, 2002.
- [15] L. Bernard, A. Ferrari, D. Micelli, A. Perotto, R. Rinaldi, and F. Vattaneo, "Electro-hydraulic valve control with multi-air technology," *MTZ worldwide*, vol. 70, no. 12, pp. 4–10, 2009.
- [16] A. Palma and C. Esposito, "The HCCI concept and control, performed with multi-air technology on gasoline engines," SAE Tech. Paper 2011-24-0026, 2011.
- [17] S. Qiao, Y. Yanding, L. Yinghao, Y. Zhi, W. Zhen, Z. Xiaoyun, and Z. Xuan, "Application of engine intelligent start-stop system in technology of vehicle fuel saving," in *Proc. 6th Int. Conf. Measuring Technol. Mechatronics Automat.*, Jan. 2014, pp. 128–131.
- [18] N. Mueller, S. Strauss, and S. Tumback, "Next generation engine start/stop systems: 'Free-wheeling,'" *SAE Int. J. Engines*, vol. 4, no. 1, pp. 874–887, 2011.
- [19] A. Shaik, N. S. V. Moorthi, and R. Rudramoorthy, "Variable compression ratio engine: A future power plant for automobiles-an overview," *Proc. Inst. Mech. Eng., D, J. Automobile Eng.*, vol. 221, no. 9, pp. 1159–1168, 2007.
- [20] M. Roberts, "Benefits and challenges of variable compression ratio (VCR)," SAE Tech. Paper 2003-01-0398, 2003.
- [21] A. C. Clenci, G. Descombes, P. Podevin, and V. Hara, "Some aspects concerning the combination of downsizing with turbocharging, variable compression ratio, and variable intake valve lift," *Proc. Inst. Mech. Eng., D, J. Automobile Eng.*, vol. 221, no. 10, pp. 1287–1294, 2007.
- [22] D. Dunn-Rankin, Ed. *Lean Combustion: Technology and Control*. New York, NY, USA: Academic, 2011.
- [23] K. Horie, K. Nishizawa, T. Ogawa, S. Akazaki, and K. Miura, "The development of a high fuel economy and high performance four-valve lean burn engine," SAE Tech. Paper 920455, 1992.
- [24] M. M. Schechter and M. B. Levin, "Camless engine," SAE Tech. Paper 960581, 1996.
- [25] M. Battistoni, F. Mariani, L. Foschini, and M. Cristiani, "A parametric optimization study of a hydraulic valve actuation system," *SAE Int. J. Engines*, vol. 1, no. 1, pp. 970–984, 2009.
- [26] Z. Sun and T.-W. Kuo, "Transient control of electro-hydraulic fully flexible engine valve actuation system," *IEEE Trans. Control Syst. Technol.*, vol. 18, no. 3, pp. 613–621, Mar. 2010.
- [27] B. M. Heisner and A. M. Croxell, "Fiat MultiAir system: Operation, diagnosis, & service," Dept. Automot. Technol., Southern Illinois Univ., Carbondale, IL, USA, 2016.
- [28] M. A. Theobald, B. Lequesne, and R. Henry, "Control of engine load via electromagnetic valve actuators," *SAE Trans.*, pp. 1323–1334, 1994.
- [29] P. Wolters, W. Salber, J. Geiger, M. Duesmann, and J. Dilthey, "Controlled auto ignition combustion process with an electromechanical valve train," *SAE Trans.*, pp. 160–168, 2003.
- [30] A. Frederic, V. Picron, J. Hobraiche, N. Gelez, and S. Gouiran, "Electromagnetic valve actuation system e-valve: Convergence point between requirements of fuel economy and cost reduction," SAE Tech. Paper, 2010.
- [31] C. Tai and T. C. Tsao, "Control of an electromechanical camless valve actuator," in *Proc. Amer. Control Conf.*, vol. 1, May 2002, pp. 262–267.
- [32] K. S. Peterson, "Control methodologies for fast and low impact electro-magnetic actuators for engine valves," Univ. Michigan, Ann Arbor, MI, USA, Tech. Rep. 3186731, 2005.
- [33] L. Liu and S. Chang, "Motion control of an electromagnetic valve actuator based on the inverse system method," *Proc. Inst. Mech. Eng., D, J. Automobile Eng.*, vol. 226, no. 1, pp. 85–93, 2012.
- [34] L. Liu and S. Chang, "A moving coil electromagnetic valve actuator for camless engines," in *Proc. Int. Conf. Mechatronics Automat.*, Aug. 2009, pp. 176–180.
- [35] P. Eyabi and G. Washington, "Nonlinear modeling of an electromagnetic valve actuator," SAE Tech. Paper 2006-01-0043, 2006.
- [36] W. S. Chang, T. A. Parlikar, M. D. Seeman, D. J. Perreault, J. G. Kassakian, and T. A. Keim, "A new electromagnetic valve actuator," in *Proc. Power Electron. Transp.*, Oct. 2002, pp. 109–118.
- [37] P. Mercorelli, K. Lehmann, and S. Liu, "Robust flatness based control of an ELA using adaptive PID controller," in *Proc. IEEE Conf. Decis. Control*, Apr. 2003, pp. 3790–3795.
- [38] S. Braune, S. Liu, and P. Mercorelli, "Design and control of an electromagnetic valve actuator," in *Proc. IEEE Conf. Comput. Aided Control Syst. Design, IEEE Int. Conf. Control Appl., IEEE Int. Symp. Intell. Control*, Oct. 2006, pp. 1657–1662.
- [39] M. Elhoseny, A. Tharwat, and A. E. Hassanien, "Bezier curve based path planning in a dynamic field using modified genetic algorithm," *J. Comput. Sci.*, vol. 25, pp. 339–350, 2018.
- [40] X. Wang, Y. Shi, D. Ding, and X. Gu, "Double global optimum genetic algorithm—particle swarm optimization-based welding robot path planning," *Eng. Optim.*, vol. 48, no. 2, pp. 299–316, 2016.
- [41] K. Deb, A. Pratap, S. Agarwal, and T. Meyarivan, "A fast and elitist multiobjective genetic algorithm: NSGA-II," *IEEE Trans. Evol. Comput.*, vol. 6, no. 2, pp. 182–197, Apr. 2002.
- [42] D. S. Weile and E. Michielssen, "Genetic algorithm optimization applied to electromagnetics: A review," *IEEE Trans. Antennas Propag.*, vol. 45, no. 3, pp. 343–353, Mar. 1997.
- [43] J. Zhao and M. Xu, "Fuel economy optimization of an Atkinson cycle engine using genetic algorithm," *Appl. Energy*, vol. 105, pp. 335–348, 2013.
- [44] G. Ma and Y. Bai, "The research and application on building a forecasting model with grey theory and neural network," *Microelectron. Comput.*, vol. 25, no. 1, pp. 153–155, 2008.
- [45] B. Su, L. Liu, and F. T. Yang, "Research of artificial neural network forecasting model based on grey relational analysis," *Syst. Eng.-Theory Pract.*, vol. 9, pp. 98–104, 2008.
- [46] C. Jin and T. Yu, "Research on monitoring and early warning of our manufacturing industrial security based on BP neural network," *J. Beijing Univ. Technol. (Social Sci. Ed.)*, to be published.
- [47] D. Niu and J. Lu, "Gray neural network forecast of power loads based on relational analysis method," *East China Electr. Power*, vol. 35, no. 8, pp. 60–62, 2007.
- [48] S. Qian, S. Zhou, and W. Chang, "A diagnosis method for diesel engine wear fault based on grey rough set and SOM neural network," in *Safety and Reliability-Safe Societies in a Changing World*. Boca Raton, FL, USA: CRC Press, 2018, pp. 995–1002.
- [49] L. Feng, "Research on the identification coefficient of relational grade for grey system," *Syst. Eng.-Theory Pract.*, to be published.
- [50] Y. Dong and Z. Duan, "A new determination method for identification coefficient of grey relational grade," *J. Xi'an Univ. Archit. Technol. (Natural Sci. Ed.)*, vol. 4, no. 40, pp. 589–592, vol. 2008.

• • •